Journal of Structural Geology, Vol. 14, No. 1, pp. 73 to 83, 1992
Printed in Great Britain

0191-8141/92 $05.00+0.00

Effect of mechanical interactions on the development of shape preferred orientations: a two-dimensional experimental approach

BENOÎT ILDEFONSE*

Geologisches Institut, ETH-Zentrum, CH-8092 Zürich, Switzerland

PATRICK LAUNEAU, JEAN-LUC BOUCHEZ

Université Paul-Sabatier, CNRS U.A. 67, Laboratoire de Pétrophysique et Tectonique, 38 rue des Trente-six Ponts, F-31400 Toulouse, France

and

ANGEL FERNANDEZ

Université de Limoges, CNRS U.A. 10, Laboratoire de Géologie Régionale et Appliquée, 123 rue Albert Thomas, F-87060 Limoges, France

(*Received* 10 *September* 1990; *accepted in revised form* 28 *May* 1991)

Abstract—Modifications in the development of preferred orientations of rigid particles due to mechanical interactions between particles are studied experimentally in two dimensions. Experiments in both pure shear and simple shear were performed and the results analysed using an easy and fast new automatic method. For increased concentration of rigid particles, the rotation of individual particles may be slowed down or even stopped due to collisions or disturbance of the flow in the matrix caused by neighbours. In coaxial flow, the fabric intensity is consequently reduced. In simple shear flow, the fabric evolution is no longer cyclic; the intensity is on average weaker and the fabric axis rotates asymptotically toward the shear plane. In the case of preferred orientations of particles having a low aspect ratio (2.5), the fabric rotates through the shear plane, then undergoes a reverse rotation and rotates toward the shear plane again. In the light of these experimental results, we emphasize that:

—quantification of finite strain based on such fabrics may lead to significant underestimates, and calculated values should be taken as minimum estimates;

—the kinematic significance of concentrated rigid particle preferred orientations in rocks is modified by interactions between particles. Techniques for qualitative or quantitative kinematic analysis may become unreliable for simple shear flows. The concentrated population fabrics show an angular behaviour close to that of passive markers: they tend to align parallel to the shear plane in simple shear flow.

INTRODUCTION

KINEMATIC inferences may be deduced in rocks from structures resulting from the partitioning of deformation, such as shape preferred orientations (SPO) defined by rigid particles. The latter has also been used for strain analysis. Since Jeffery (1922), many theoretical and experimental studies have considered the mechanical behaviour of rigid particles and the development of shape fabrics, but few have considered the problem of the possible effects of interactions between the particles on their rotation and thus on the development of SPO. Some experimental works in fluid mechanics have dealt with these effects in three-dimensional simple shear flow (Mason & Manley 1957, Anczurowski & Mason 1967, Anczurowski *et al.* 1967). Fluid mechanicists have shown that concentrated rigid particle suspensions reach steady-state preferred orientations only after a very large number of particle rotations (3000 in Mason & Manley 1957). Consequently, application of these results to SPO in rocks, which frequently involve quite concentrated populations of particles, is not easy because the accumulated shear strains are not as large as in experimental studies in fluid mechanics. Because of the comparatively low finite strain in most rocks (Pfiffner & Ramsay 1982), geologists are more interested in what happens in the early stages of rigid particle fabric evolution, corresponding to the first few periods of rotation in simple shear (see theory below). Mason & Manley (1957, p. 129) demonstrated that interaction between two rigid rods causes a disturbance in their period of rotation, but no theory describes this effect. In order to describe the effect of interaction under conditions that can be extrapolated to a first approximation to fabrics in rocks, two-dimensional experimental tests of the influence of rigid particle concentration on the development of SPO have been performed in simple shear flow (Ildefonse & Fernandez 1988) and coaxial flow. The effect of rigid particle interactions upon both orientation and intensity of experimentally-produced SPO is presented here and implications for the significance of rigid particle fabrics are discussed.

*Present address: Laboratoire de Tectonophysique, U.S.T.L., Place Eugène Bataillon, 34060 Montpellier Cédex, France.

BACKGROUND

Theory

In a suspension of rigid particles within a viscous matrix, the flow is locally accommodated by spinning of the particle. Equations of the rotation rate in two dimensions are given by many authors (e.g. Gay 1968, Reed & Tryggvason 1974, Ghosh & Ramberg 1976, Fernandez 1984). The preferred orientation of a set of initially randomly oriented particles may be represented by the fabric ellipse. The quadratic extensions of the principal axes of this ellipse characterize the intensity of the fabric or 'density' (with the density maximum D_M along the major axis) and are given by the eigenvalues (and their orientation by the eigenvectors) of the 'orientation tensor' obtained from the direction cosines of the particles in the chosen reference frame (Harvey & Laxton 1980).

In homogeneous coaxial flow, assuming no area change, non-interacting rigid particles rotate with an angular velocity depending on their shape (i.e. their aspect ratio), so that the corresponding fabric ellipse is related to the applied strain ellipse by the equation (see Fernandez 1981, 1984 for further details):

$$D_M = \lambda_1^K, \qquad (1)$$

where K is the shape factor $(n^2 - 1)/(n^2 + 1)$ of the particles, with n as their aspect ratio, and λ_1 is the principal quadratic extension (equal to the axial ratio in two dimensions) of the strain ellipse. In two dimensions, the maximum density D_M is equal to the axial ratio R_F of the fabric ellipse (Fig. 1).

In homogeneous simple shear flow, a rigid particle rotates periodically, the period depending on the particle aspect ratio (Ghosh & Ramberg 1976, Fernandez *et al.* 1983). Thus, the fabric of a population composed of equally shaped particles with an initial random distribution also evolves periodically. The fabric passes through a maximum of intensity ($D_{M_{max}} = n^2$) when its axis coincides with the shear direction ($\alpha = 0$; Fig. 2). At this instant, the instantaneous angular velocity is a minimum and the corresponding 'critical shear strain' γ_c (Fig. 2) is given by the equation (see Fernandez *et al.* 1983 for further details):

$$\gamma_c = \pi/\sqrt{1 - K^2}. \qquad (2)$$

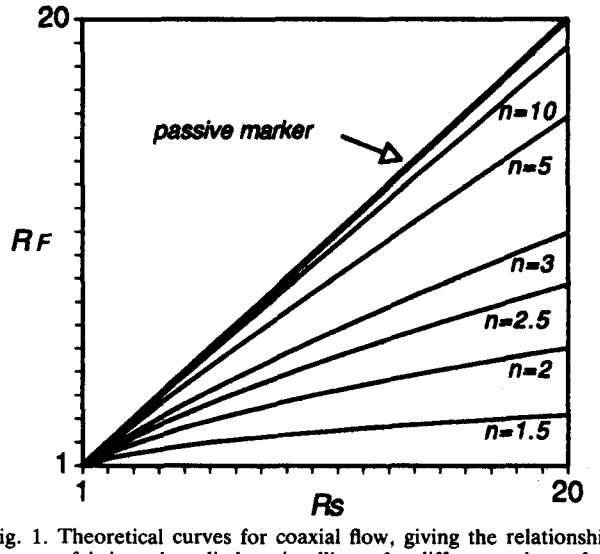

Fig. 1. Theoretical curves for coaxial flow, giving the relationships between fabric and applied strain ellipses for different values of the rigid particle aspect ratio n (equation 1 in text). R_s is the axial ratio of the finite strain ellipse (equal to λ_1 in two dimensions); R_F is the axial ratio of the fabric ellipse. The curve for a fabric defined by passive markers is given for reference. For a given applied strain, fabric intensity decreases with decreasing n.

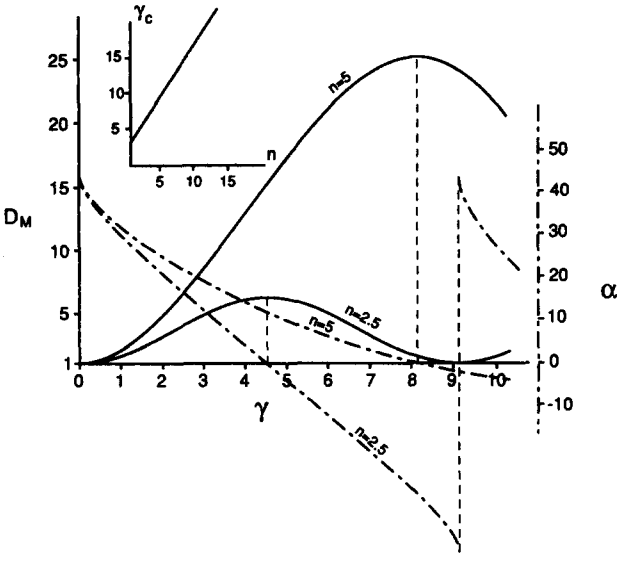

Fig. 2. Theoretical curves for simple shear flow, giving the fabric intensity (maximum density D_M; solid lines) and fabric orientation (α; dash-dot lines) as a function of the shear strain (γ) for rigid particles of aspect ratio $n = 2.5$ and 5. The upper left-hand diagram gives the critical shear strain (γ_c) as a function of n (equation 2 in text). Because of its cyclic evolution, the fabric axis passes instantaneously from $\alpha = -45°$ to $\alpha = +45°$ (with respect to the shear plane) when its intensity is minimum.

Experiments

The homogeneous simple shear box is described in Fernandez *et al.* (1983); it was inspired by those of Taylor (1934) and Willis (1977). The homogeneous pure shear apparatus is described in Fernandez (1984). In the two systems, the viscous matrix was a mixture of clear honey with titanium oxide, the latter allowing some viscosity control (about 50–70 Pa s) and giving a white matrix necessary for a good photographic contrast. Rigid particles, cut from a thin PVC sheet, were homogeneously distributed and oriented on the surface of the matrix. The high viscosity contrast between particles and matrix and the slow applied strain rate ($<2 \times 10^{-3}$ s^{-1}) allowed the theoretical rotation law, linearly related to the applied strain tensor, to be respected (Jeffery 1922). Several runs were performed with equal shaped particles ($n = 2.5$ or 5) and a single one with a mixed population ($n = 2.5$ and 5). Various initial concentrations were tested, the particles undergoing collisions when their mutual distances became less than their length. The experimental data were collected as photo-

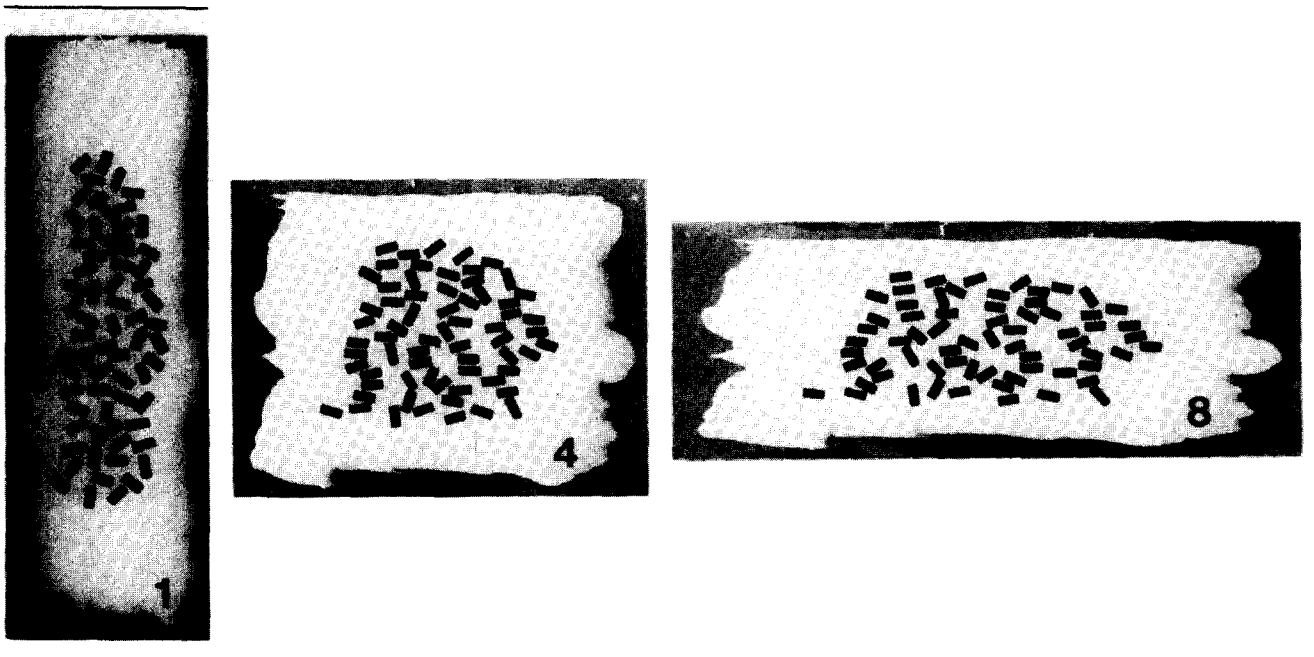

Fig. 4. Example of a progressive pure shear run with a high-concentration population of $n = 2.5$ markers. The number in the lower right-hand corner is the axial ratio of the applied strain ellipse (R_s).

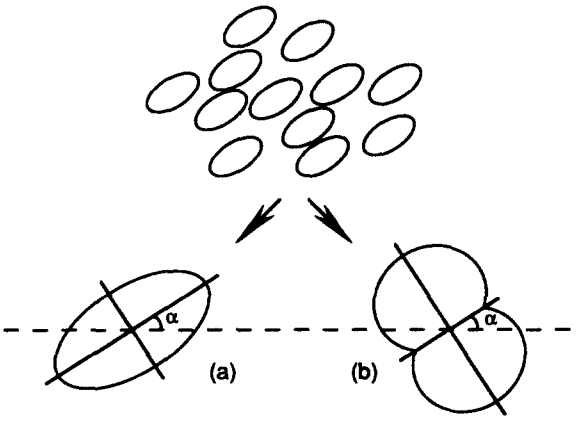

Fig. 3. Correspondence between (a) the fabric ellipse and (b) the rose of intercepts for a population of passive elliptical markers.

graphs of successive strain increments during each experiment.

Data treatment

The data have been treated using the method described in detail in Launeau *et al.* (1990). This automatic parametric method involves digitization of an image with a CCD camera and separation of the considered object population from its matrix. The analysis then consists of counting the intercepts between a rotating grid and the image. The angle α of the SPO is the one for which the number of intercepts is minimum (Fig. 3), the principal axes of the 'intercept rose' being calculated using the eigenvector method. The degree of preferred orientation (fabric intensity) is related to the ellipticity index I_e of the intercept rose, which measures the departure from a circle: 1 − (1/axial ratio of the intercept rose).

For comparison, the experimental data were also treated using the classical eigenvalue method (Harvey & Laxton 1980) for which the operator has to identify each particle defining the fabric. By contrast, the automatic method, which analyses the particle–matrix system globally, allows a rapid and easy treatment of fabrics without requiring any operation other than driving the computer in the image filtering procedure. As a consequence, the main difference between the axial eigenvalue method and the intercept method is that the latter takes into account the particle shape in addition to particle orientation (Panozzo 1983, Launeau *et al.* 1990). Departure from the ideal elliptical shape is the source of noticeable variations in the shape and consequently in the axial ratio of the intercept rose (the axial ratio of a rectangular particle is underestimated by about 4%, Launeau *et al.* 1990). In the case of passive markers, the intercept rose, as the fabric ellipse (see Harvey & Laxton 1980), is directly related to the strain ellipse (Fig. 3). In the case of rigid particles, both methods result in identical fabric orientation; however, the axial ratio of the intercept rose is not equal to the axial ratio of the fabric ellipse obtained with the eigenvalue method. The maximum value that the axial ratio of the intercept rose can attain, in the ideal case of parallelism of all the particles, is the average aspect ratio of the particles (for further discussion, see Launeau *et al.* 1990, pp. 209–210). Thus, the relationship between the intercept rose and the strain ellipse remains to be inferred in the case of a population of rigid particles. This might be done by calibrating the intercept method against the classical eigenvalue method.

EXPERIMENTAL RESULTS

Pure shear flow

Experiments have been performed with various concentrations of rigid particles. For more clarity, we have distributed these experiments into two groups: the low-concentration experiments are those for which there was no contact between the particles; in the high-concentration experiments (Fig. 4), as many as 40% of the total population of particles undergo collisions with neighbours. Figure 5 shows that, at a given finite strain, the degree of preferred orientation, given by the ellipticity index, is always lower in high-concentration experiments. Decrease in fabric intensity is, therefore, related to the concentration of particles: mechanical interactions between particles tend to block or slow down their rotation toward some equilibrium. On the other hand, note that changing the concentration of particles does not affect the orientation of the fabric: in coaxial flow, the fabric initiates always parallel to the

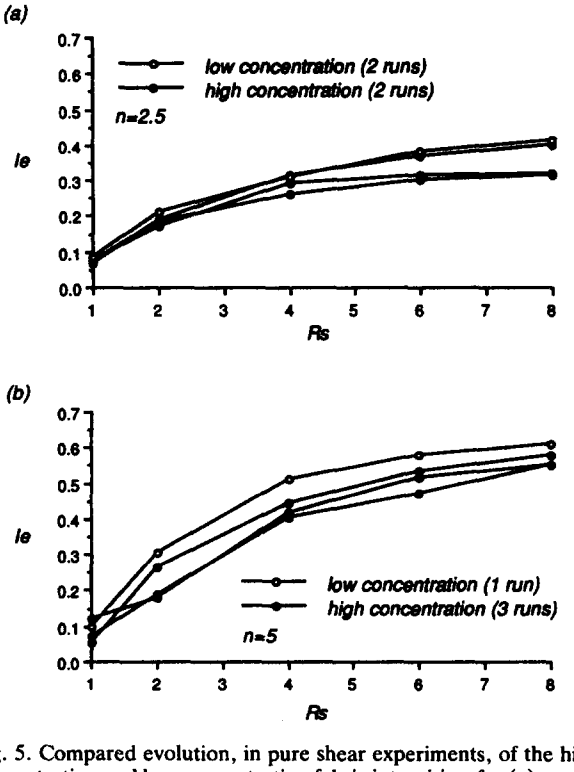

Fig. 5. Compared evolution, in pure shear experiments, of the high-concentration and low-concentration fabric intensities, for (a) $n = 2.5$ and (b) $n = 5$. I_e = ellipticity index of the intercepts rose; R_s = axial ratio of the applied strain ellipse.

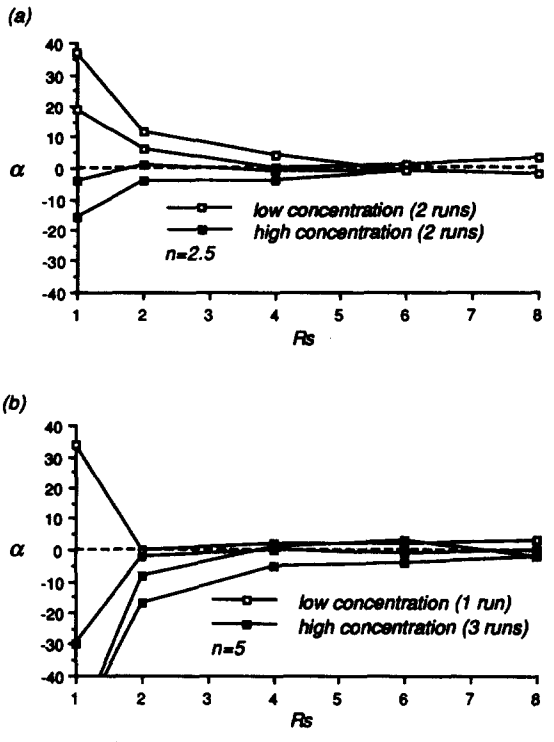

Fig. 6. Compared evolution, in pure shear experiments, of the high-concentration and low-concentration fabric orientations, for (a) n = 2.5 and (b) n = 5. α = fabric orientation; R_s = axial ratio of the applied strain ellipse. The fabric initiates parallel to the maximum elongation direction; the observed deviation from this ideal behaviour is due to the slight anisotropy of initial populations, acting on the orientation as a pre-existing fabric.

maximum elongation direction and does not change orientation as deformation progresses (Fig. 6).

Simple shear flow

Experiments in simple shear flow were presented and discussed in Ildefonse & Fernandez (1988). We present here a more detailed analysis of some experiments for a better understanding of the role of mechanical interactions between particles.

In the low-concentration experiments, the fabric behaviour satisfied the theoretically predicted one, except for slight deviations inherent to these experiments, due to an initial departure from a perfect homogeneous orientation distribution and/or to the small number of particles affecting the overall statistics (Fig. 7).

In experiments with higher particle concentrations, the fabric no longer evolves periodically (Fig. 8). Its intensity is on average weaker than in the case of diluted populations and shows smaller variation (compare Figs. 7a and 8a); the minimum intensity remains higher than in low-concentration experiments. This decrease in average intensity is even larger with more elongated (n = 5) particles (Ildefonse & Fernandez 1988). The effect of interactions between particles on the fabric orientation is more spectacular: the periodicity of the fabric with increasing strain is lost. The fabric axis rotates toward the shear plane and then remains sub-parallel to it, in the range of ±10°. In the experiments with shorter particles (n = 2.5), a reverse rotation of the fabric axis is observed (Fig. 8b). In an experiment with a mixed population (n = 2.5 and 5), the n = 2.5 sub-fabric shows the same reverse rotation while the n = 5 sub-fabric rotates progressively toward the shear plane with a constant sense of rotation (Fig. 9). When n = 5, the fabric axis always rotates more slowly in high-concentration experiments than in ones with lower concentrations (Ildefonse & Fernandez 1988); in addition, as in Fig. 9(a) (n = 5), the α vs γ curve never cross-cuts the shear plane.

The observed reverse rotation of the fabric (n = 2.5 and concentrated populations) could be due to reverse rotation of at least a part of the particle population, i.e. anticlockwise rotation in our dextral simple shear experiments. In order to check this, the sense of rotation of each particle has been determined for each increment in the high-concentration experiment ss27 (n = 2.5). Some particles do rotate anticlockwise during one or several successive increments, this reverse rotation being associated with collision with neighbours (Fig. 10a). Anticlockwise rotations of particles rarely exceed a few degrees, however, and the percentage of anticlockwise rotating particles never exceeds 17% (Fig. 10b). Because the slight reverse rotations of some particles cannot alone account for the important reverse rotation of the fabric axis (Figs. 8 and 9), the latter must be

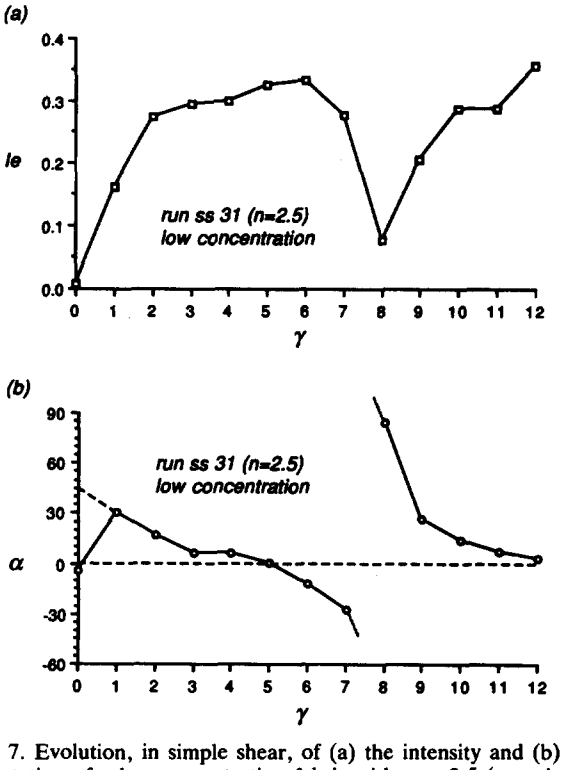

Fig. 7. Evolution, in simple shear, of (a) the intensity and (b) the orientation of a low-concentration fabric with n = 2.5 (experiment ss31, 13 particles). In (b) the dashed part of the curve shows what would be the evolution of the fabric if the initial distribution were truly random (fabric initiation at 45° to the shear plane). The dotted part of the curve links cycle 1 to cycle 2 of the fabric, where the intensity is minimum; theoretically, intensity should be momentarily null, the fabric should disappear with its axis oriented at −45° and immediately re-appear with its axis oriented at 45°. Departure from this ideal behaviour is due to the non-perfectly uniform initial distribution and to the low number of particles. I_e = ellipticity index of the intercepts rose, γ = applied shear strain.

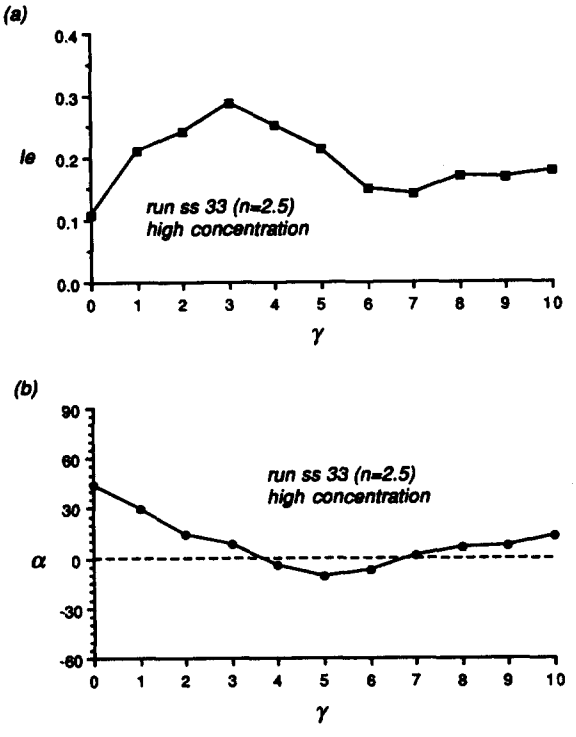

Fig. 8. Evolution, in simple shear, of (a) the intensity and (b) the orientation of a high-concentration fabric with $n = 2.5$ (experiment ss33, 132 particles). I_e = ellipticity index of the intercepts rose; γ = applied shear strain.

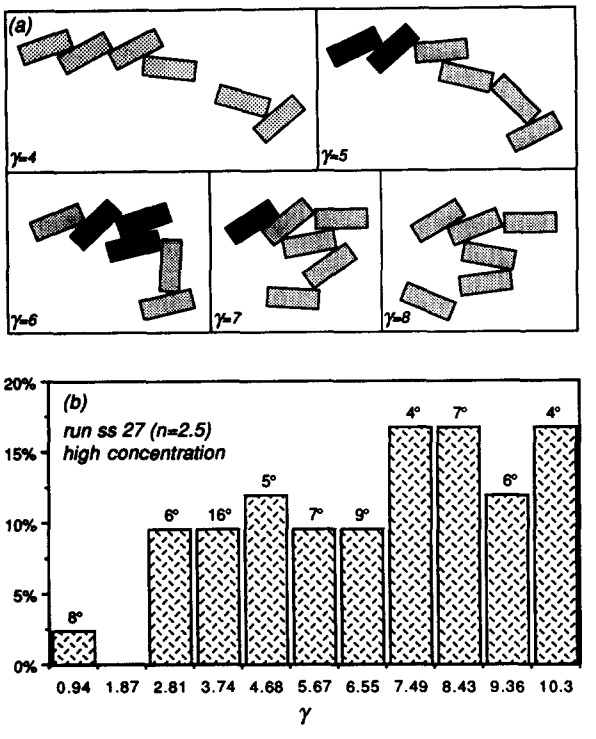

Fig. 10. (a) Detailed sketch of the formation and evolution of a cluster in a dextral simple shear high-concentration experiment. Darkened markers are those undergoing reverse rotation during the corresponding increment. (b) Percentage of particles rotating anticlockwise in each increment for the high-concentration simple shear experiment ss27 (80 particles). The average anticlockwise rotation is given for each increment.

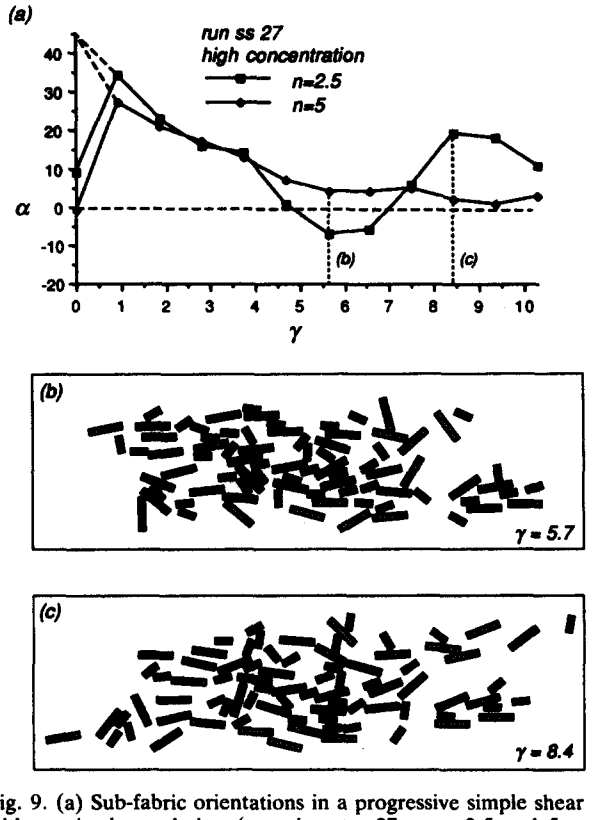

Fig. 9. (a) Sub-fabric orientations in a progressive simple shear run with a mixed population (experiment ss27, $n = 2.5$ and 5, with, respectively, 41 and 39 particles). Dashed curves: same significance as in Fig. 7. (b) Sketch of the fabric at $\gamma = 5.7$. (c) Sketch of the fabric at $\gamma = 8.4$.

considered as apparent. This effect is explained by the varying rotation rates of sub-populations, due to mechanical interactions between particles.

Varying rotation rates due to interactions

We observed that rotation of clusters of particles is systematically slowed or even blocked because of interactions, the latter being either true collisions or disturbance of the flow in the matrix due to neighbours. A well-known interaction feature among rotating rigid particles is the so-called 'tiling effect' in which particles arrange themselves as tiles on a roof (see for examples Figs. 9 and 10a) (Fernandez *et al.* 1983, Blumenfeld & Bouchez 1988, Ildefonse & Fernandez 1988, Benn & Allard 1989). These clusters may behave for a while like single aggregate particles that rotate more slowly because they are more elongate than the individual particles. This effect, together with temporary blocking of some particles and flow disturbances, is responsible for the slowing down of part of the population as in Figs. 4, 9 and 10 (see also fig. 2 in Ildefonse & Fernandez 1988). Hence, because part of the population of particles follows a slower rotation cycle, more particles are rotating toward the shear plane ($\alpha > 0$) than particles rotating away from the shear plane ($\alpha < 0$). This situation is illustrated in Fig. 11(a) for two high-concentration populations. For comparison, a similar graph from a low-concentration experiment (Fig. 11b) shows a pattern much closer to what is expected with an ideally uniform initial distri-

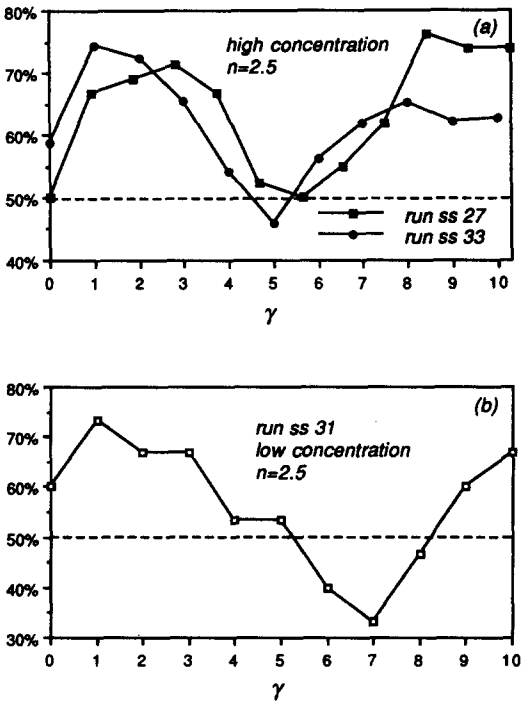

Fig. 11. Percentage of particles positively oriented ($\alpha > 0$, axes trending toward the shear plane) in (a) two high-concentration experiments (ss33, 132 particles and ss27, 80 particles) and (b) one low-concentration experiment (ss31, 13 particles), in simple shear. γ = applied shear strain.

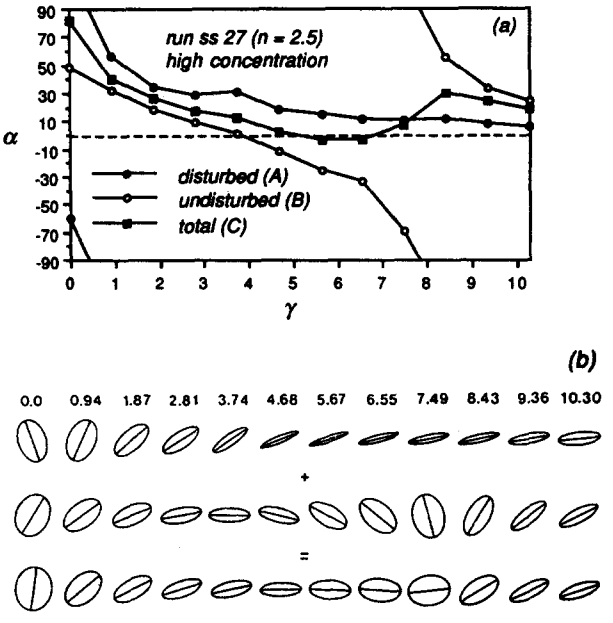

Fig. 12. Experiment ss27, fraction $n = 2.5$, 41 particles. (a) Orientation curves for the two sub-fabrics corresponding respectively to disturbed and undisturbed particles (see text) compared to the total fabric orientation curve and (b) corresponding sequences of finite fabric ellipses. The disturbed sub-fabric (A, 36% of the total $n = 2.5$ population) shows a behaviour close to the $n = 5$ fabric (see Fig. 9a); the undisturbed sub-fabric (B, 64% of the total $n = 2.5$ population) shows a behaviour close to the low-concentration $n = 2.5$ fabric (see Fig. 7b). For better clarity, ellipses were drawn with constant length in order to align corresponding increments in the three sequences; area changes have no physical significance. As in Fig. 7, the departure from the theoretical behaviour (fabrics should initiate at 45°, disappear and reappear at −45° and 45°, respectively) is due to the non-perfectly random initial distribution and to the low number of particles.

bution and no interactions. Theoretically, this pattern should be symmetrical and centred on the 50% line; intersection with this line should correspond to instants when the fabric is null ($\gamma = 0, 9.11, \ldots$ for $n = 2.5$) or a maximum ($\gamma_c = 4.55, \ldots$ for $n = 2.5$). The influence of interactions on the apparent reverse rotation of the fabric can also be shown by separating the population of particles into two sub-populations (Fig. 12): in sub-population A, each particle has undergone a rotation smaller than 90° during the experiment; in sub-population B, each particle has undergone a rotation larger than 90°. In this way, we separate the particles which were highly disturbed by interactions from those which were undisturbed or only slightly disturbed by interactions. Plots of the two corresponding sub-fabrics, compared to the total one (Fig. 12), illustrate how the disturbed particles modify the behaviour of the total fabric: the disturbed sub-fabric (A) remains positively oriented ($\alpha = 0$) while the undisturbed one (B) begins a new cycle at $\gamma \approx 8$.

In order to test what size (number of particles) of a sub-population shows this phenomenon, another analysis was performed on partial populations which were selected from restricted areas of the same experiment ss27 (Fig. 13). The sub-areas correspond to 45 and 25% of the nominal area of the experiment, providing approximately 55 and 30 particles, respectively. As expected, the accuracy of measurements for both orientation and intensity of the sub-fabrics is worse in the smallest areas because of the lower number of particles. Nevertheless, the results demonstrate that, for the γ range considered in this experiment, the relative patterns for the two sub-fabrics ($n = 2.5$ and 5) remain constant whatever the size of the measured populations. Therefore, we suggest that the effect of mechanical interactions between rigid particles is local and more or less the same whatever the number of particles.

DISCUSSION

The image processing technique of Launeau *et al.* (1990), based on the treatment of the intercept function, is very powerful for fabric analysis in a rock as long as the particles may be distinguished by the filtering procedure. A given crystal species (here the dark particles) can be rather easily isolated from its matrix (here the white medium) for data analysis. As the parametric method is not adapted to shape recognition of individual particles, the fabric of a given crystal species will be analysed globally. Analysis of sub-fabrics, such as in Fig. 13 ($n = 2.5$ vs $n = 5$), therefore needs a previous separation of the sub-populations.

Note that we only refer to 'low-concentration' and 'high-concentration' populations and do not propose a threshold for the concentration of particles under which interactions would not produce a significant effect. As a matter of fact, we do not have a precise idea of the minimum distance under which two rigid particles will interact. Because of flow disturbance around rotating

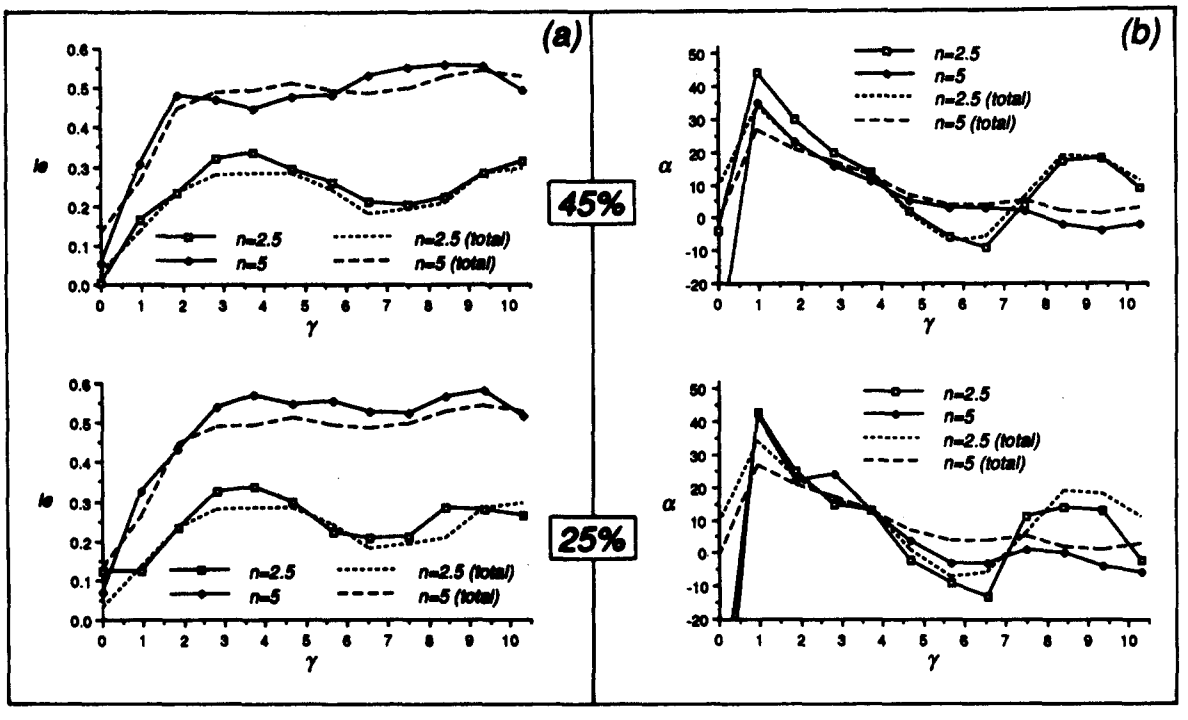

Fig. 13. Evolution of (a) intensity and (b) orientation of the sub-fabrics in experiment ss27 (80 particles) when analysing smaller areas. The curves obtained on the total experiment area (Fig. 9a) are given in dashed and dotted lines for comparison. The sizes of the areas are given as a percentage of the total in the rectangular boxes (45 and 25%; corresponding, respectively, to 55 and 30 particles on average). As in Figs. 7 and 12, the departure from the theoretical behaviour (fabrics should initiate at 45°, disappear and reappear at −45° and 45°, respectively) is due to the non-perfectly random initial distribution and to the low number of particles.

rigid particles, we just emphasize that interactions occur at a distance larger than the average particle length. Calculation of a critical distance will most likely depend on several parameters, such as particle size and shape, amount of accumulated finite strain, flow vorticity, etc. The existing estimates in the literature are quite empirical (e.g. Burgers 1938, Mason & Manley 1957) and a detailed study still needs to be done. One must also note that in three dimensions, because of the additional degree of freedom for particle motion, description of the effect of interactions might be even more complex. For example, oblate and prolate objects with similar aspect ratios would probably show different interaction patterns.

Strain analysis using rigid particle fabrics is one of the goals of our study. In the case of non-interacting particle fabrics, the intensity is theoretically related to finite strain in coaxial flow (equation 1) (Fernandez 1988), or in simple shear flow with elongate particles ($n > 5$; Ildefonse & Fernandez 1988). In both pure shear and simple shear, it is clearly shown from this current work that the fabric intensity decreases with increasing particle concentrations. Therefore, the strain values obtained from populations with interacting particles will be systematically underestimated.

Most important for geological studies of deforming rocks is the use of rigid particle fabrics for kinematic analysis (e.g. Fernandez *et al.* 1983, Passchier 1987, Vissers 1989). However, because of modified rotation rates of particles when interactions occur, the kinematic significance of rigid particle fabrics is also modified. As a consequence, in non-coaxial flow, quantification of the vorticity number (Passchier 1987) will give non-significant results using concentrated populations. Comparisons between sub-fabrics within mixed populations may also not be as safe as theoretically predicted. For example, the reverse rotation of fabric axes (Figs. 8 and 9), will contradict the theoretical angular relationship between sub-fabrics which was shown to be a good shear criterion by Fernandez *et al.* (1983). Thus, although it has been clearly demonstrated that this criterion may be valid in natural igneous rocks (e.g. Benn & Allard 1989), the only systematically safe method for concentrated populations remains the analysis of tiled clusters (Blumenfeld & Bouchez 1988). An important result of interactions in simple shear flow is that a better and more stable alignment of the fabric axis with the shear plane is expected. This alignment is especially good in the case of more elongate particles ($n = 5$, Fig. 9) but occurs for more equant particles as well ($n = 2.5$, Fig. 12). Primary igneous foliation or other fabrics, when defined by concentrated populations of rigid particles are therefore expected to be very close to the shear plane for high shear strain values ($\gamma \geq 5$).

CONCLUSION

The effect of mechanical interactions on the development of two-dimensional rigid particle fabrics has been experimentally investigated in both coaxial and non-coaxial (simple shear) homogeneous flows.

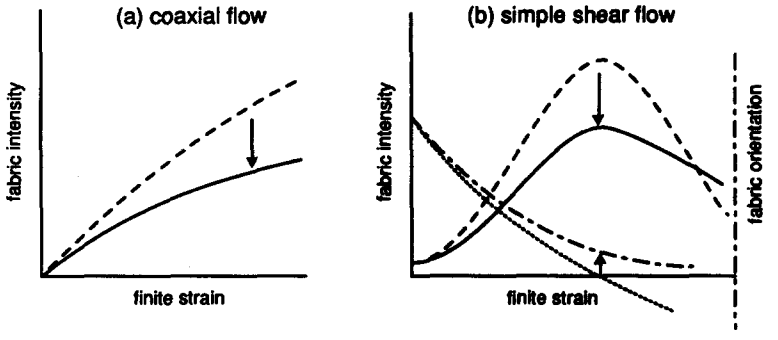

Fig. 14. Schematic effect of increasing mechanical interactions between rigid particles on fabric development for (a) coaxial and (b) simple shear flows. Trends are given by the arrows from the low-concentration case (dashed and dotted curves) to the high-concentration one (solid and dash-dot curves); they are more pronounced for higher aspect ratios.

The experimental results have been treated using an automatic image analysis technique (Launeau *et al.* 1990). It allows rapid and easy analysis of SPO, mainly because the tedious work of identifying and measuring the individual particles is avoided. Compared to the axial-eigenvalue method (Harvey & Laxton 1980) previously used (Ildefonse & Fernandez 1988), this new method is significantly faster without affecting the accuracy (see the tests in Launeau *et al.* 1990). However, the methods do not quantify strain in the same way. The axial method directly calculates the fabric ellipse from the axial angular distribution of the particles while the intercept method integrates information on both orientation and shape of the rigid particles. Thus, in ideal situations of diluted populations where strain measurements would be meaningful, the intercept method should be calibrated against the classical axial-eigenvalue method.

The effect of mechanical interactions between rigid particles is mostly to slow down particle rotation. In pure shear flow, the fabric is weakened for a given finite strain magnitude (Fig. 14a). In simple shear flow, the fabric intensity is also weaker on average but, as the cyclic evolution tends to disappear, it never attains the null value predicted for low-concentration suspensions (Fig. 14b). The corresponding fabric axis approaches the shear plane more slowly, remains close to it and never crosses it as theoretically predicted (Fig. 14b). Whatever the flow regime, the decrease in intensity is observed to be stronger for the higher aspect ratios ($n = 5$). The 'reverse rotation' of the fabric axis observed in runs with $n = 2.5$ is clearly due to mechanical interactions and cannot be attributed to the observed slight reverse rotations of some particles. It is explained by the different rotation rates (or periods) of sub-populations (interacting and non-interacting particles; Fig. 12). Within mixed populations (particles with different aspect ratios), the angular relationships between sub-fabrics are shuffled, and the sense of shear criterion derived from the sub-fabrics is no longer reliable.

In rocks, especially igneous ones, suspensions of rigid particles may be quite concentrated. SPO development is then expected to be similar to that described in the present experiments. Finite strain computations should, therefore, always be taken as minimum values; qualitative and quantitative kinematic analysis, which is always based on angular relationships between different objects (Passchier 1987, Vissers 1989) or between different populations or sub-populations (Fernandez *et al.* 1983), must be done with great care. Conversely, the SPO of such suspensions will tend to remain sub-parallel to the shear plane for high accumulated shear strains. At a high aspect ratio ($n = 5$), this angular behaviour is more effective and approaches that for passive markers. The SPO is then useful in discussing the direction of regional-scale motions (see discussions in Burg *et al.* 1987, Ildefonse & Caron 1987). It must be pointed out, however, that the sub-parallelism with the shear plane observed in our experiments will probably not occur in non-coaxial flows differing significantly from simple shear, because in flows between pure shear and simple shear the orientation for minimum angular velocity of rigid particles is not parallel to the shear plane (Ghosh & Ramberg 1976, Ildefonse *et al.* 1990). Experimental investigation of fabric development in such flows remains to be done.

Acknowledgements—We gratefully acknowledge Peter Hudleston, Neil Mancktelow, Lisa Dell'Angelo and two anonymous reviewers for their careful review. Jean-Michel Caron is thanked for reviewing an early version of the manuscript. This paper was written while Benoît Ildefonse was a postdoctoral fellow at ETH-Zürich, funded by Swiss National Fond Grant No. 21-25258.88. Experiments were performed in UCB Lyon I, France, with support from the CNRS U.A. 726. Patrick Launeau and Jean-Luc Bouchez thank the CNRS U.A. 67 for general support and the INSU for participating in the numerical image analysis equipment.

REFERENCES

Anczurowski, E., Cox, R. G. & Mason, S. G. 1967. The kinetics of flowing dispersions. IV. Transient orientations of cylinders. *J. Colloid Interface Sci.* **23**, 547–562.

Anczurowski, E. & Mason, S. G. 1967. The kinetics of flowing dispersions. III. Equilibrium orientations of rods and discs (Experimental). *J. Colloid Interface Sci.* **23**, 533–546.

Benn, K. & Allard, B. 1989. Preferred mineral orientations related to magmatic flow in ophiolite layered gabbros. *J. Petrol.* **30**, 925–946.

Blumenfeld, P. & Bouchez, J.-L. 1988. Shear criteria in granite and migmatite deformed in the magmatic and solid states. *J. Struct. Geol.* **10**, 361–372.

Burg, J.-P., Bale, P., Brun, J.-P. & Girardeau, J. 1987. Stretching lineations and transport direction in the Ibero-Armorican arc during the Siluro-Devonian collision. *Geodin. Acta* **1**, 71–87.

Burgers, J. M. 1938. On the motion of small particles of elongated form suspended in a viscous liquid. *Vehr. K. ned. Akad. Wet.* **16**, 113–184.

Fernandez, A. 1981. Une généralisation du modèle de March applicable à l'analyse des orientations préférentielles de forme issues de la déformation coaxiale dans les roches éruptives. *C. r. Acad. Sci. Paris* **293**, 1091–1094.

Fernandez, A. 1984. Etude théorique et expérimentale du développement de la fabrique dans les roches magmatiques. Application à l'analyse structurale des granitoïdes. Unpublished thèse ès Sciences, Clermont-Ferrand.

Fernandez, A. 1988. Strain analysis from shape preferred orientation in magmatic rocks. In: *Geological Kinematics and Dynamics (in Honor of the 70th Birthday of Hans Ramberg). Bull. geol. Instn Univ. Uppsala* **14**, 61–67.

Fernandez, A., Feybesse, J. L. & Mezure, J. F. 1983. Theoretical and experimental study of fabric developed by different shaped markers in two-dimensional simple shear. *Bull. Soc. geol. Fr.* **25**, 319–326.

Gay, N. C. 1968. Pure shear and simple shear deformation of inhomogeneous viscous fluids. I—Theory. *Tectonophysics* **5**, 211–234.

Ghosh, S. K. & Ramberg, H. 1976. Reorientation of inclusions by combination of pure shear and simple shear. *Tectonophysics* **34**, 1–70.

Harvey, P. K. & Laxton, R. R. 1980. The estimation of finite strain from the orientation distribution of passively deformed linear markers; eigenvalue relationships. *Tectonophysics* **70**, 285–307.

Ildefonse, B. & Caron, J.-M. 1987. The significance of stretching lineations in terms of progressive deformation and finite strain. *Geodin. Acta* **1**, 161–170.

Ildefonse, B. & Fernandez, A. 1988. Influence of the concentration of rigid markers in a viscous medium on the production of preferred orientation. An experimental contribution, 1. Non-coaxial strain. In: *Geological Kinematics and Dynamics (in Honor of the 70th Birthday of Hans Ramberg). Bull. geol. Instn Univ. Uppsala* **14**, 55–66.

Ildefonse, B. Lardeaux, J.-M. & Caron, J.-M. 1990. The behaviour of shape preferred orientations in metamorphic rocks: amphiboles and jadeites from the Monte Mucrone area (Sesia-Lanzo zone, Italian Western Alps). *J. Struct. Geol.* **12**, 1005–1011.

Jeffery, G. B. 1922. The motion of ellipsoidal particles immersed in a viscous fluid. *Proc. R. Soc. Lond.* **102**, 161–179.

Launeau, P., Bouchez, J. L. & Benn, K. 1990. Shape preferred orientation of object populations: automatic analysis of digitized images. *Tectonophysics* **180**, 201–211.

Mason, S. G. & Manley, R. S. 1957. Particle motion in sheared suspension: orientations and interactions of rigid rods. *Proc. R. Soc. Lond.* **238**, 117–131.

Panozzo, R. 1983. Two-dimensional analysis of shape-fabric using projections of digitized lines in a plane. *Tectonophysics* **95**, 279–294.

Passchier, C. W. 1987. Stable positions of rigid objects in non-coaxial flow—a study in vorticity analysis. *J. Struct. Geol.* **9**, 679–690.

Pfiffner, O. A. & Ramsay, J. G. 1982. Constraints on geological strain rates: arguments from finite strain states of naturally deformed rocks. *J. geophy. Res.* **87**, 311–321.

Reed, L. J. & Tryggvason, E. 1974. Preferred orientation of rigid particles in a viscous fluid matrix deformed by pure shear and simple shear strain. *Tectonophysics* **24**, 85–98.

Taylor, G. I. 1934. The formation of emulsion in deformable fields of flow. *Proc. R. Soc. Lond.* **A146**, 501–523.

Vissers, R. L. M. 1989. Asymmetric quartz *c*-axis fabrics and flow vorticity: a study using rotated garnets. *J. Struct. Geol.* **11**, 231–244.

Willis, D. G. 1977. A kinematic model of preferred orientation. *Bull. geol. Soc. Am.* **88**, 883–894.